Chemineer

How to disperse gases in liquids

André Bakker
Chemineer, Inc.

John M. Smith
University of Surry

Kevin J. Myers
University of Dayton

HOW TO DISPERSE GASES IN LIQUIDS

Concave-blade disc impellers provide the right mix of shear and flow for better mass transfer in gas-liquid systems

André Bakker
Chemineer Inc.

John M. Smith
University of Surrey

and Kevin J. Myers
University of Dayton

Mixing of a gas in a liquid is required in fermentation operations and a variety of oxygenation and hydrogenation processes. Agitation increases the mass transfer between the gas and the liquid phase. Gas-liquid reactors equipped with agitators are often operated at high power input and large gas holdup, making these units among the most difficult to design.

For gas-dispersion applications, an impeller system must perform many tasks. For example, the system has to create large velocity gradients, or shear rates, to break the gas into small bubbles. High levels of turbulence are needed to decrease the mass-transfer resistance between the gas and the liquid phase. Finally, the impeller system has to provide sufficient flow to maintain overall uniformity of the mixture. Modern high-efficiency [1] and concave-blade disc impellers (Figure 1) provide the proper balance of flow, turbulence and shear for most applications.

For an overview of the state of the art in gas-liquid agitation, a number of excellent reports are available [2, 3]. This article aims to present practical design guidelines while explaining the basics of gas-liquid mixing. It expands on design procedures presented in 1976 by Hicks and Gates [4] and capitalizes on recent advances in flow-visualization techniques [5], development of new gas-dispersion impellers and improved understanding of the dispersion process itself.

Methods to calculate power draw, gas holdup and mass-transfer rate are illustrated with examples. It is shown that concave-blade turbines provide better performance than the traditional flat-blade units.

New developments in design

In the 1970s, it was usual to specify radial-flow, flat-blade turbines (Figure 2) for gas-dispersion applications. Since then, however, several new impeller designs have become available. The advent of concave-blade disc impellers has had an impact on gas-liquid agitation in much the same way as high-efficiency impellers have affected liquid blending [1] and solids suspension [6]. Several variations on the concave-blade disc turbine are available commercially. Moreover, a number of large chemical companies make inhouse versions of these impellers.

Multiple impeller systems using a combination of radial-flow impellers mounted below axial-flow, high-efficiency impellers are also becoming increasingly popular. These impeller systems can maintain a more uniform dissolved-oxygen concentration, which is especially important in biological reactor systems, such as fermenters. Figure 3 shows the single-phase flow pattern in such a reactor as calculated with the aid of computational fluid dynamics (CFD) modeling software.

MULTI-IMPELLER ARRANGEMENT	
Z_g/T	Number of impellers
< 0.9	1
0.9–1.7	2
1.7–2.5	3
2.5–3.3	4

TABLE 1. The recommended number of impellers is a function of Z_g/T

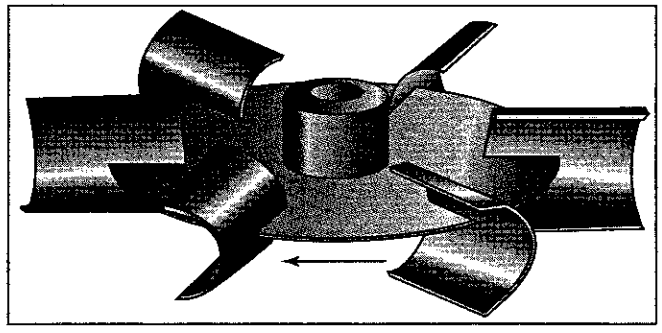

FIGURE 1. A concave-blade turbine provides the right amount of turbulence, shear and flow for most gas-liquid mixing applications

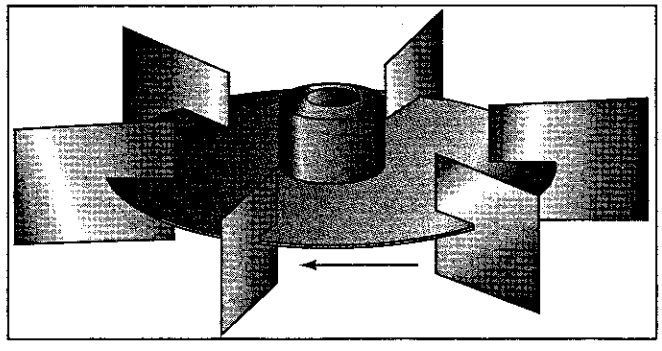

FIGURE 2. Flat-blade turbines have long been specified for gas-dispersion applications, but now impellers of alternative designs are offering better performance

DEBORAH LEVITT

With such multi-impeller arrangement, the gas sparger should be mounted below the radial-flow impeller. The radial-flow impeller breaks up the gas bubbles effectively while the upper high-efficiency impeller ensures circulation and bulk mixing of the vessel contents. This impeller configuration works especially well when there is relatively little bubble coalescence.

The recommended number of impellers for gas dispersion depends on the ratio of the gassed-liquid level, Z_g, to the tank diameter, T, as outlined in Table 1. For optimum performance, the impellers need to be separated from each other by a distance at least equal to the smallest impeller diameter. The impeller sizes are usually chosen such that the diameter of the high-efficiency impellers is about 1.3 times that of the radial turbine. This arrangement gives the optimum distribution of the input power throughout the vessel. The ratio of impeller diameter to tank diameter (D/T) should be between 0.3 and 0.5 for radial turbines and between 0.4 and 0.65 for high-efficiency impellers.

Gas-dispersion systems with a bottom radial-flow impeller and upper high-efficiency impellers are preferred for biological systems. However, units with multiple radial-flow impellers can sometimes outperform mixed radial- and axial-flow impeller systems in nonbiological processes. The preferred gas-sparger arrangement is a ring sparger mounted below the lowest impeller with a diameter between 0.5 and 0.75 times the diameter of the impeller.

It is best to use four baffles. The baffle width should be 1/12th the tank diameter. Dead spaces are reduced if the baffles are mounted at 1/6th the baffle width from the wall. Baffles should extend from the vessel's bottom tangent line to the liquid surface. If the liquid level is variable, extend the baffles to the upper tangent line.

Patterns of gassed-liquid flows

The flow pattern in a gas-liquid reactor determines the homogeneity of the dispersion that influences the gas holdup, the mass transfer rate and the local dissolved-gas concentrations. The flow regimes for single radial-flow turbines are shown in Figure 4.

For a given gas flowrate, the flow pattern in the tank depends on the agitator speed. At low impeller speeds, the action of the impeller may be overwhelmed by the rising gas flow. Under these conditions, the impeller is "flooded" because the gas rises directly through the impeller to the liquid surface (Figure 4A). An increase in impeller speed at fixed gas flow leads to a situation where the impeller disperses the gas radially. This situation is usually referred to as "loading" when the gas bubbles reach the vessel wall, but do not recirculate below the impeller.

If the impeller speed is increased further, the gas eventually recirculates throughout the whole of the tank volume. The impeller speed at which this complete dispersion occurs is designated N_{cd}. Increasing the impeller speed beyond this point does not change the overall flow pattern in the tank. The increase in agitation intensity, however, leads to an increase in gas holdup and mass-transfer rate.

Along with variations in the overall flow pattern are changes in the flow around the impeller blades. Figure 5 shows the flow generated by a radial-flow turbine at various gas flowrates while the impeller speed is kept constant. At low flowrates, the gas is entrained in the vortices behind the impeller blade. With increasing gas flow, the size of the cavities increases to the point that the cavities begin to cling to the rear of the blade. At even higher gas flowrates, a series of large cavities develops (Figure 6).

A flat-blade disc turbine forms alternately larger and smaller cavities, generally referred to as the "3-3 structure." When the gas flow is increased beyond the flooding point, the regularity of the cavity structure is lost and other cavity shapes develop [2, 3].

The overall flow patterns and cavity shapes for a concave-blade turbine are similar to those generated by flat-blade turbines. However, the onset of cavity formation occurs at higher gas flowrates. Also, the cavities tend to be smaller with a concave-blade turbine, leading to a smaller drop in power demand upon gassing. As a result, this impeller can disperse significantly more gas at a given speed and diameter than the flat-blade turbine.

In the turbulent regime, the gassed

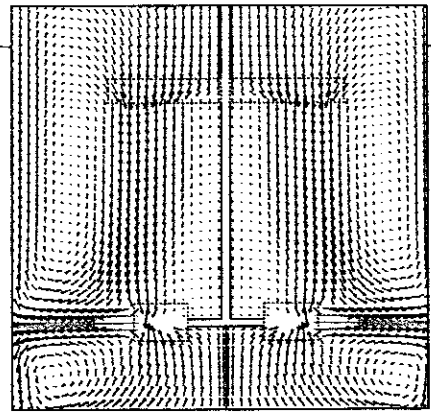

FIGURE 3. The flow pattern in a reactor equipped with a radial-flow turbine at the bottom and a high-efficiency, axial-flow impeller at the top is calculated with CFD modeling software. Red and blue denote high and low velocities, respectively

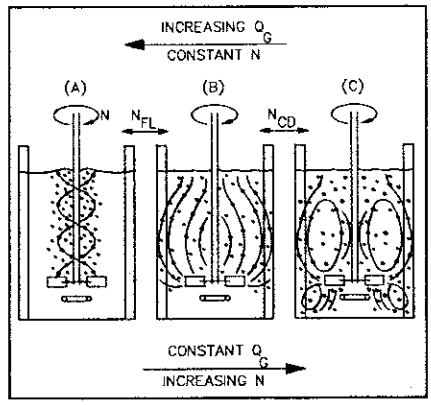

FIGURE 4. The various flow regimes in a gassed stirred tank equipped with a radial-flow turbine. A represents flooded impeller. B indicates how the impeller disperses the gas outwards to the wall. In C, the gas is completely dispersed. When the impeller speed N is increased while the gas flowrate Q_g is kept constant, the flow pattern changes in the order from A to B to C. When the impeller speed is kept constant and the gas flowrate is increased, the flow pattern changes in the order: C to B to A

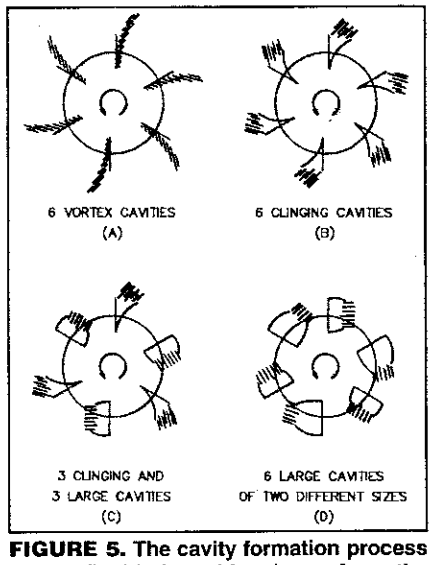

FIGURE 5. The cavity formation process with a flat-blade turbine (seen from the bottom of a tank) affects the overall flow pattern in the tank

EFFECT OF IMPELLER TYPE ON POWER NUMBER	
Impeller type	N_p
Flat-blade disc turbine	5.50
Concave-blade turbine	3.20
High-efficiency impeller	0.32

TABLE 2. The power number in the turbulent-flow regime is a function of the impeller type

flow pattern depends primarily on two dimensionless variables, namely the aeration number and the Froude number. The aeration number, N_A, is proportional to the ratio of the gas flowrate to the pumping capacity of the impeller.

$$N_A = \frac{Q_g}{ND^3} \quad (1)$$

The Froude number, N_{Fr}, is a measure of the ratio of inertial to gravitational forces.

$$N_{Fr} = \frac{N^2 D}{g} \quad (2)$$

The maximum aeration number for water at which flooding occurs, can be calculated from [7]:

$$N_{A,FL} = C_{FL} N_{Fr} \left(\frac{D}{T}\right)^{3.5} \quad (3)$$

For a flat-blade turbine, C_{FL} = 30, and for a concave-blade turbine, C_{FL} = 70. Equation 3 shows that at the same speed and diameter the concave-blade impeller can handle more than twice the gas flowrate of the flat-blade impeller before being flooded.

These equations are based on work by Warmoeskerken and Smith [7]. The performance of a concave-blade turbine depends on the curvature of the blades. Recent work by Sensel [8] has shown that the equations for the concave-blade turbine represent conservative estimates for impellers with half-cylinder blades, which have a minor effect on $N_{A,FL}$. Nevertheless, Equation 3 presents an easy-to-use guideline.

An increase in viscosity slightly decreases the gas-handling ability of the flat-blade impeller, but has little effect on the transition to flooding with the concave-blade impeller. This is another plus for the concave-blade impeller.

Combining the equations developed by Nienow [3] and Warmoeskerken and Smith [7] for air-water systems, leads to the following equation for the transition to a flow pattern where the gas is completely dispersed:

$$N_{A,CD} = C_{CD} \left(\frac{D}{T}\right)^{0.5} N_{Fr}^{0.5} \quad (4)$$

In the above equation, C_{CD} = 0.2 for a flat-blade turbine, and C_{CD} = 0.4 for a concave-blade turbine. The gas is dispersed from gas-filled cavities behind the impeller blades. The minimum Froude number that must be exceeded if the turbine is to retain any of the cavities needed to achieve a gas-dispersing regime is given by:

$$N_{Fr,min} = 0.045 \quad (5)$$

for both flat- and concave-blade impellers. Below this value for the Froude number, the gas cannot be satisfactorily dispersed, independent of the gas flowrate. The minimum aeration number to develop large cavities is given by:

$$N_{A,LC} = C_{LC} D^{0.2} \left(\frac{D}{T}\right)^{-0.5} \quad (6)$$

Here C_{LC} = 0.025 for a flat-blade turbine, and C_{LC} = 0.058 for a concave-blade turbine. Equations 3 through 6 can be plotted in flow maps (Figure 7), showing the flow regimes as a function of N_A and N_{Fr}. Two lines for each impeller show the transitions to flooding and completely dispersed states.

Such a map is simple to prepare and provides an easy-to-use tool to determine the flow regime. This map also indicates that the concave-blade turbine can handle higher gas flowrates than the flat-blade turbine before flooding. For all gas-dispersion applications, the regimes yielding flooding conditions should be avoided.

The situation in a tank equipped with multiple impellers is slightly different. If the impellers are not flooded, the gas rising from the region agitated by the lowest impeller is distributed across the tank and does not affect the

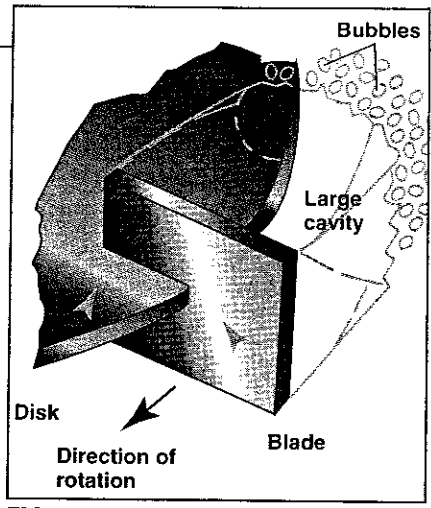

FIGURE 6. A large gas-filled cavity forms behind the blade of a flat-blade turbine with increasing gas flow

NOMENCLATURE

Symbols	Meaning
a	Interfacial area per unit volume, m^{-1}
c_l	Concentration of soluble gas in liquid, mol/m^3
c_l^*	Saturation concentration of soluble gas in liquid, mol/m^3
C_a	Constant
C_{kla}	Constant
C_{CD}	Constant
C_{FL}	Constant
C_{LC}	Constant
D	Impeller diameter, m
g	Acceleration due to gravity, m/s^2
k_L	Liquid side mass transfer coefficient, m/s
MTR	Mass transfer rate, $mol/s \cdot m^3$
N	Impeller rotational speed, s^{-1}
N_A	Aeration number
N_{Fr}	Froude number
N_p	Impeller power number
N_{Re}	Reynolds number
N_{CD}	Impeller speed at completely dispersed transition, s^{-1}
$N_{A,CD}$	Aeration number at completely dispersed transition
$N_{A,FL}$	Aeration number at flooding transition
P_g	Gassed power consumption, W
P_u	Ungassed power consumption, W
Q_g	Actual gas flowrate, m^3/s
T	Tank diameter, m
v_{sg}	Superficial gas velocity, m/s
V_g	Volume of gas, m^3
V_l	Volume of liquid, m^3
Z_g	Liquid level under gassed conditions, m
Z_u	Liquid level under ungassed conditions, m
α	Gas holdup
μ	Dynamic viscosity, Pa·s
ρ	Density, kg/m^3

CONSTANTS FOR EQUATION 9				
Blade type	a	b	c	d
Flat	0.72	0.72	24	0.25
Concave	0.12	0.44	12	0.37

TABLE 3. Equation 9 provides the gassed power draw for radial turbines mounted directly above a gas sparger

upper impellers to the same extent as it would if the same volume were supplied from a sparger. Consequently, the upper impellers are almost never flooded by the gas.

The flow regime around the bottom impeller is generally similar to those for a single impeller (Figure 4). The upper impellers usually work in a bubbly regime that corresponds to fully dispersed conditions.

Calculating power requirements

The power drawn by an impeller strongly correlates with the cavity formation process and the associated gassed-flow pattern. With an increase in cavity size, the power draw of the impeller decreases (Figure 8). The relative power demand (that is, the ratio of the gassed power draw, P_g, to the ungassed power draw, P_u) is a function of the aeration number at constant Froude number. The shape of such gassed power curves depends on the impeller Froude number. The effect of gassing on power draw is less pronounced for the concave-blade turbine than it is for the flat-blade impeller.

When designing an agitator drive, one needs to calculate both the ungassed and gassed power draws. The ungassed power draw of an impeller can be calculated from:

$$P_u = N_p \rho N^3 D^5 \tag{7}$$

The power number is a function of the impeller Reynolds number, N_{Re}.

$$N_{Re} = \frac{\rho N D^2}{\mu} \tag{8}$$

If the flow generated by the impeller is fully turbulent (N_{Re} > 10,000), the impeller power numbers are constant (Table 2). For low Reynolds numbers (below 10,000), the power numbers may be different from the values listed here. However, most gas-liquid applications are fully turbulent.

The gassed power draw, P_g, of radial turbines mounted directly above a gas sparger can be calculated from Equation 9 using Table 3.

$$P_g = P_u(1-(b-a\mu)N_{Fr}^d \tanh(cN_A)) \tag{9}$$

The power draw of upper high-efficiency impellers that are not mounted directly above a gas sparger can be calculated from:

CASE STUDY

Problem: A recently built reactor, equipped with a flat-blade disc turbine, does not satisfy the process requirements. By examining the liquid surface, the operator suspects that the gas is rising straight through the impeller to the liquid surface. In other words, the impeller is flooded. The mass-transfer rate is usually lower when the impeller is flooded than when it is able to completely disperse the gas. The information about the reactor is listed in Table 4.

Solution: From Equation 3, one can calculate the aeration number at which the impeller is flooded. For the present example, $N_{A,FL}$=0.13. The impeller operates at N_A= 0.21, which is significantly greater than the aeration number at which the flat-blade turbine is flooded. This confirms the suspicion of the operator that the impeller is flooded. The flooding can also be anticipated from the flow regime map in Figure 7. Poor gas dispersion is most likely the cause of the unsatisfactory performance of the reactor.

To prevent the impeller from flooding, the gas flowrate can be decreased. However, this is undesirable because reduced gas flowrate leads to a lower mass-transfer rate. Therefore, it is decided to replace the flat-blade turbine with a concave-blade turbine that can handle larger gas flowrates. The gassed power draw of the flat-blade turbine is calculated with Equation 9 to be 1,540 W.

At the given gassing rate, a 0.84-m-dia. concave-blade turbine turns out to draw the same power. Recalculating the aeration number and the Froude number shows that this impeller is not flooded: N_{Fr}= 0.12; and N_A at 0.18 is less than $N_{A,FL}$ at 0.37. Thus, replacing the 0.80-m flat-blade turbine with a 0.84 m concave-blade turbine solves the flooding problems in the reactor. □

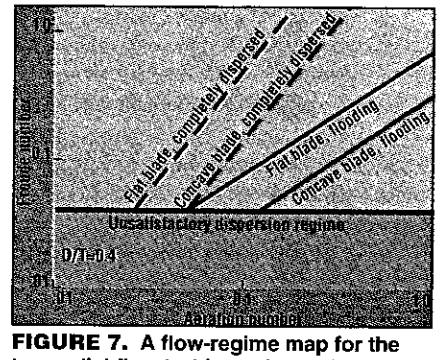

FIGURE 7. A flow-regime map for the two radial-flow turbines shows the transitions to flooding and completely dispersed states

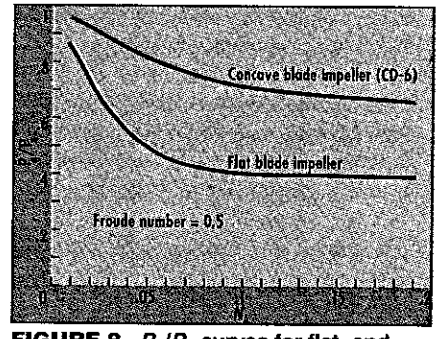

FIGURE 8. P_g/P_u curves for flat- and concave-blade turbines show the dependence of relative power demands on impeller types

MAKEUP OF A REACTOR

Parameters	Values
T	2.0 m
D	0.80 m
N	1.13 s^{-1}
Q_g	0.12 m^3/s
μ	0.001 Pa·s
ρ	1,000 kg/m^3
N_A	0.21
N_{Fr}	0.10

TABLE 4. The given operating parameters have led to gas flooding in the reactor

$$\begin{aligned} P_g &= P_u(1-(a+bN_{Fr})N_A^{c+0.04N_{Fr}}) \\ a &= 5.3\exp(-5.4(D/T)) \\ b &= 0.47(D/T)^{1.3} \\ c &= 0.64 - 1.1D/T \\ 0.40 &< D/T < 0.65 \\ 0.5 &< N_{Fr} < 2 \\ 0.05 &< N_A < 0.35 \end{aligned} \tag{10}$$

It is usually more economical to design large agitator drives such that the motor is fully loaded under gassed conditions. However, appropriate safety precautions must be taken to prevent the motor from overloading when the gas flow is interrupted. This overloading is less of a problem with the concave-blade impeller, whose power draw is less sensitive to gassing.

Often, it is possible to drive the agitator with a two-speed motor. In this case, the agitator can operate at the high speed when gassed, and at the low speed when ungassed.

Optimizing gas holdup

Gas holdup is an important design parameter. Not only does it have a direct influence on the mass-transfer rate, but an increased holdup may raise the liquid level or decrease the amount of liquid a tank can hold. The gas holdup is defined as:

$$\alpha = \frac{V_g}{V_g + V_l} = \frac{Z_g - Z_u}{Z_g} \tag{11}$$

Gas holdup is a function of the physical properties of the liquid, the impeller system, the power input and the gas rate. It can be predicted by the following correlation:

$$\alpha = C_\alpha \left(\frac{P_g}{V_l}\right)^A v_{sg}^B \quad (12)$$

For water-air systems agitated with a single impeller, the following constants can be used:

$$C_\alpha = 0.16 \pm 0.04$$
$$A = 0.33 \quad (13)$$
$$B = 0.67$$

In this correlation, the gas flowrate is expressed in terms of the superficial gas velocity, v_{sg}.

$$v_{sg} = \frac{Q_g}{\frac{\pi}{4}T^2} \quad (14)$$

The values of the constants in Equation 12 depend on the reactor geometry, the impeller type and the physical properties of the fluid. Generally, concave-blade turbines give a larger gas holdup than flat-blade turbines. However, the differences are within the accuracy margin of measurements of the constants in Equation 13.

For other fluids and for multiple-impeller systems, the constants C_α, A and B should be measured on a small-scale system that is geometrically similar to the largescale reactor. Equation 12 can then be used to predict the gas holdup on the large scale, provided that the tanks are operated in the non-flooded regime. When the constants cannot be measured, Equation 12 can still be used because at constant superficial gas velocity and power per unit mass, the gas holdup also remains constant.

Enhancing mass-transfer rate

Transferring mass from the gas phase to the liquid phase is the main goal of most gas-liquid mixing applications. The mass transfer rate is given by:

$$MTR = k_L a(c_l^* - c_l) \quad (15)$$

The volumetric mass-transfer coefficient, $k_L a$, has been the subject of many studies. Many correlations have been presented in the literature. The most successful correlations express $k_L a$ in terms of the superficial gas velocity and the power input per unit volume:

$$k_L a = C_{kla}\left(\frac{P_g}{V_l}\right)^a v_{sg}^b \quad (16)$$

The constants can be dramatically influenced by liquid properties. Further, such contaminants as surfactants and insoluble oils can have a strong effect on $k_L a$.

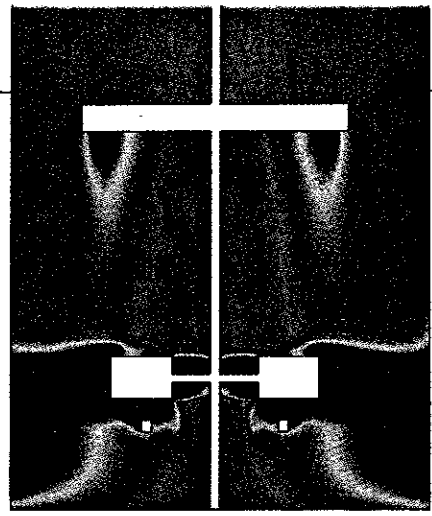

FIGURE 9. $k_L a$ maps for reactor systems provide useful insight into the mass-transfer processes. Red and blue denote regions with high and low mass-transfer rates, respectively

Equation 16 holds only when the impeller is not flooded and should be used as a scaleup correlation in a way similar to the holdup correlation. The constants can be measured on a small scale with the actual process fluids in a tank that is geometrically similar to the largescale production tank.

For air-water systems equipped with single impellers, the following constant can be used, with a= 0.6 and b = 0.6:

$$C_{kla} = 0.015 \pm 0.005 \quad (17)$$

These constants are averages, based on several hundred experiments with many different impeller types. Although the constants depend on impeller type, the variation in $k_L a$ for different impellers is usually within 30% around the average. At high gas flowrates, concave-blade impellers can provide mass transfer rates at least 20% higher than flat-blade impellers.

The equations presented above for holdup and mass transfer provide overall values. Given that it is impossible to obtain fully homogeneous gas-liquid dispersions, large variations in the local gas holdup and the local mass-transfer rate can occur, regardless of the agitation intensity. When knowledge of the local mass-transfer rate is important, for example, to prevent microorganism starvation, the gas-liquid dispersion should be analyzed with the aid of simulation software for computational fluid dynamics (CFD).

The results from CFD simulation for the local mass-transfer coefficient, $k_L a$, are shown in Figure 9. Simulations like this provide valuable insight into the underlying processes. More discussions about CFD techniques can be found elsewhere [5].

The design steps to follow

The rules given above for flow regime, power consumption, gas holdup and mass-transfer rate allow the design of largescale gas-liquid reactors. The correct procedure is to specify a required gas holdup or mass-transfer rate based on process experience. Then an economical combination of power consumption and gas rate must be found that satisfies the process demands.

Further, the impeller must be capable of dispersing the gas. Usually, this will require several iterative steps through the equations presented above. Another option is to first optimize the process in a small-scale reactor and then scale it up to industrial size. ■

Edited by G. Sam Samdani

References

1. Fasano, J. B., and others, Advanced Impeller Geometry Boosts Liquid Agitation, *Chem. Eng.*, Aug. 1994, pp. 110–116.
2. Smith, J. M., Dispersion of Gases in Liquids, in "Mixing of Liquids by Mechanical Agitation," (ed. by Ulbrecht, J. J., and Patterson, G. K.), Gordon and Breach Science Publishers, 1985, pp. 139–202.
3. Nienow, A. W., Gas Dispersion Performance in Fermentor Operation, *Chem. Eng. Progress*, Feb. 1990, pp. 61–71
4. Hicks, R. W., and Gates, L. E., How to Select Turbine Agitators for Dispersing Gas into Liquids, *Chem. Eng.*, July 19, 1976, pp. 141–148.
5. Bakker, A., and others, Pinpoint Mixing Problems with Lasers and Simulation Software, *Chem. Eng.*, January 1994, pp. 94–100.
6. Corpstein, R. R., and others, The High-Efficiency Road to Liquid-Solid Agitation, *Chem. Eng.*, Oct. 1994, pp. 138–144.
7. Warmoeskerken, M. M. C. G., and Smith, J. M., The Hollow Blade Agitator for Dispersion and Mass Transfer, *Chem. Eng. Res. Des.*, 67 (3), 1989, pp. 193–198
8. Sensel, M. E., "Gas Dispersion at High Aeration Rates in Low to Moderately Viscous Newtonian Liquids," M. Sc. Thesis, University of Dayton, Ohio, 1992.

The authors

John M. Smith has been BOC professor of chemical and process engineering at the University of Surrey at Guildford in England since 1987, following 16 years as professor of physical technology at the Technical University of Delft in the Netherlands. His research interests center on mixing in multiphase and complex systems with particular interest in process hydrodynamics. He holds M.Sc. and D.Sc. degrees in chemical engineering from the University of Manchester (U.K.).

For biographical information on **André Bakker** and **Kevin J. Myers,** see CE, January, p. 100, and October, p. 144, respectively.